

## RESEARCH ARTICLE

# Design of a PV-fed electric vehicle charging station with a combination of droop and master-slave control strategy

Divya Krishnan Nair  | Krishnamachar Prasad | Tek T. Lie

School of Engineering, Computer and Mathematical Sciences, Auckland University of Technology, Auckland, New Zealand

## Correspondence

Divya Krishnan Nair, School of Engineering, Computer and Mathematical Sciences, Auckland University of Technology, Auckland, New Zealand.  
Email: [divya.krishnan.nair@autuni.ac.nz](mailto:divya.krishnan.nair@autuni.ac.nz)

## Funding information

School of Engineering, Computer and Mathematical Sciences, Auckland University of Technology, Auckland, New Zealand

## Abstract

Electric vehicles (EVs) are becoming essential elements for both the transport and power sectors. Consequently, they need a suitable charging infrastructure at the same time. Electric vehicle charging stations (EVCS) assisted by photovoltaic (PV) panels draw attention due to minimal expenditure, increased environmental awareness, and a consistent increase in the effectiveness of the PV modules. In this paper, a combination control scheme utilizing the merits of both droop and master-control strategies for the EVCS is proposed. In addition, an isolated bidirectional DC-DC converter combined with the snubber circuits and a three-level boost converter that utilizes a capacitance-voltage control design is used to further enhance the system stability. The design of the EVCS is formulated and validated through MATLAB/Simulink.

## KEYWORDS

bidirectional converter, droop control, electric vehicle charging station, master-slave control, photovoltaic, snubber circuit

**Abbreviations:** A, ampere; AC, alternating current; CO<sub>2</sub>, carbon dioxide; DC, direct current;  $D_C$ , duty ratio generated from capacitor voltage;  $D_{PV}$ , duty ratio generated from solar panels; ESU, energy storage unit; EV, electric vehicle; EVCS, electric vehicle charging station;  $G'$ , slope of solar irradiance;  $G_{avg}$ , disable function based on the average sun irradiance; GHG, greenhouse gases; ICE, internal combustion engines; IEA, international energy agency;  $I_{ESU-ref}$ , storage current reference;  $I_{EV-ref}$ , reference charging current; IGBT, insulated gate bipolar transistor;  $K_{ESU}$ , ESU droop gain; MATLAB, matrix laboratory; MOSFET, metal-oxide-semiconductor field-effect transistor; MPPT, maximum power point tracking; MW, megawatt;  $P_{ESU}$ , ESU power;  $P_{EV}$ , maximum consumption from the EVs; PI, proportional integral controller;  $P_{mpp}$ , maximum output power from the PVs; PV, photovoltaic; SOC, state-of-charge; V, voltage; V2G, vehicle to grid;  $V_{PV}$ , solar panel voltage;  $V_{ref}$ , reference voltage; W, watts;  $\Delta I_{EV}$ , droop control's output.

## 1 | INTRODUCTION

Electric vehicles (EVs) has led to a paradigmatic change in the electric and transportation sectors. In recent years, EVs have become a viable alternative due to the transport sector's contribution of 23% to worldwide emissions of greenhouse gases (GHG) connected to energy. The percentage of renewable energy used in transportation is quite low currently but is experiencing a tremendous transformation, especially in the wagon category where EVs are gaining ground.<sup>1</sup> According to the IEA reports, the number of electric vehicles sold worldwide reached 10 million in the year 2020. The greatest fleet is in China, where there are 4.5 million electric vehicles, but in 2020, Europe saw the largest yearly growth, rising to 3.2 million. If most cars built after 2040 are electric, more than

This is an open access article under the terms of the [Creative Commons Attribution-NonCommercial-NoDerivs](https://creativecommons.org/licenses/by-nc-nd/4.0/) License, which permits use and distribution in any medium, provided the original work is properly cited, the use is non-commercial and no modifications or adaptations are made.

© 2023 The Authors. *Energy Storage* published by John Wiley & Sons Ltd.

1 billion people might have access to EVs by 2050.<sup>2</sup> Electricity is an ideal low-cost fuel for the transportation sector due to the cost reduction in renewable energy generation. The increasing deployment of EVs provides a great scope for the power sector as these vehicles have the potential to reduce emissions and save energy. EVCS has the potential to provide massive amounts of storage capacity for electricity. Uncontrolled charging of EVs on the grid might result in system overload, thus necessitating upgrades to the distribution and transmission as well as in the generation capacity.<sup>3,4</sup> Private investments are necessary to develop charging infrastructure, but currently, few business models make sense for them. Government can provide incentives for the installation of EVCS in both residential and public access areas. Furthermore, a crucial and ongoing challenge is to optimize the charging, aggregation, and overall management of EVs on the grid. As a result, crucial decisions about where to place charging points, which technologies to utilize, and to optimize slow smart charging and rapid charging to best serve consumers will have to be addressed while establishing charging infrastructure.<sup>5</sup>

The demand for charging infrastructure is projected to rise as the number of electric vehicles grows, placing additional strain on the grid. EV charging patterns are unpredictable and erratic, as well as the rising deployment of rapid charging systems that take significant grid power for shorter durations exacerbates this situation.<sup>4,6</sup> Major and costly renovations will be required for both the transmission and distribution systems, as well as associated components of the energy network. The impact of EV charging on the low voltage network was investigated by Zou et al<sup>7</sup> who discovered that overloading on the transformers had a detrimental impact on the power quality. To safeguard the network, grid charging points must manage EV charge characteristics like time and demand for charging when they arrive at a charging point. These responses, on the other hand, are unpredictable and difficult to assess.<sup>8</sup> Girard et al<sup>9</sup> found that charging EVs via the grid has no environmental benefits. Using the off-grid method to charge EVs, on the other hand, results in a significant reduction in CO<sub>2</sub> emissions. As a result, building stand-alone off-grid charging stations would be an ideal approach for promoting EV adoption globally while minimizing the impact on the current power grid.<sup>10</sup>

In an earlier publication,<sup>11</sup> it has been shown that an off-grid EVCS using PV energy can be effectively installed in remote locations. The most common renewable sources of energy are solar and wind. However, wind energy consists of multiple conversion stages to produce power compared to PV energy. Therefore the feasibility of PV-based EVCS is more attractive.

Compared with more common AC grid-connected EV charging stations, the benefits of DC off-grid connected EVCS include the following<sup>12,13</sup>:

- Minimal energy conversion losses in systems that include DC sources.
- Continuous supply of high-quality power and free from skin effect and reactive power losses.
- Less expensive and fewer power-electronic gadgets.
- No need to consider utility grid synchronization.

So, there is a great trend in PV-fed DC fast-charging stations in the literature. A typical PV-fed DC fast charging station consists of solar arrays, EV chargers, energy storage unit (ESU), and numerous DC-DC power converters. A microgrid charging station may offer charging facilities in remote areas. Multiple applications have made use of off-grid charging stations. The world's biggest off-grid solar project, the DeGrussa Solar farm in Australia, uses a 10.6 MW solar PV panel and a 6 MW battery system to supplement a 23 MW diesel-fired power station, saving an estimated 5 million liters of diesel fuel each year. It also saves 12 million tons of CO<sub>2</sub> emissions. Since 2017, Robben Island has been cut off from the mainland's electricity system; however, it is equipped with a 666.4 kW solar PV system and a battery energy storage microgrid. It may save 275 000 gal of diesel every year, and 820 t of CO<sub>2</sub> emissions are eliminated from the air each year, helping to protect the island's ecosystem and wildlife.<sup>14</sup>

The published work on PV-based charging systems covers system design, vehicle-to-grid (V2G) operations, power management, and electricity bill reduction in smart homes.<sup>15-21</sup> Because all these methods involve a greater standard over a long duration, they cannot tolerate unexpected system perturbations such as rapid irradiance shifts. It has been demonstrated by Thang et al<sup>22</sup> that a sliding-mode control can be used to enhance the robustness of the output voltage of the DC bus to bridge this gap. However, the coordination of EVs and ESU is absent. To prevent the ESU from being overcharged and overdischarged, Wu et al<sup>23</sup> develop a coordinated control in the islanded mode. Although, there is no evidence of transient PV generating interruption that would compromise system stability. According to Xia et al,<sup>24</sup> a decentralized control system for synchronizing solar power with ESU charging/discharging is proposed. They employ a droop control-based technique for the ESU, and adaptive power regulation for the PV generator. Furthermore, the EV chargers were depicted simplistically and were not included in the synchronization. This prevented any investigation into the impact of failures on the EV side.

Global EV makers have increased their investments to create and market contemporary EV models because of concerns over climate change, the shortage of fossil fuels, and advances in battery technology. Compared to cars powered by ICEs, EVs produce much fewer GHG emissions. Most nations have started to encourage the use of electric vehicles by implementing specific programs like tax incentives, reduced parking fees, etc. Range anxiety, often known as the restricted range with a fully charged battery, is one of the key issues preventing customers from converting to EVs. The range typically ranges from 100 km to 500 km. A battery may be recharged in anywhere from 30 minutes to 10 hours, depending on the quality of the charging stations. By offering a charge duration of between 30 and 60 minutes, installed fast charging stations distributed in appropriate areas might alleviate this issue. The features of the charger circuit affect the battery charging profile, including the charging time, battery life, and efficiency. The charger circuit's functionality is influenced by the type, components, control strategies, switching methods, and total cost of the converter implementation. The control circuit should be easy to construct and versatile.<sup>25</sup> Therefore, the isolated bidirectional DC-DC converter in the ESU's control circuit is snubber-equipped and is used to regulate the battery's charging and discharging. Since the leakage inductance and low voltage side-fed inductor currents have different current densities, this form of system layout clamps the rail voltage, reducing current spikes at the converter's switches.

However, depending on the electricity generation source, the charging stations have their own drawbacks, including the overloading of the current grid infrastructure and the potential to drastically increase carbon emissions. The development of an off grid charging infrastructure coupled with PV panels is the appropriate remedy to address the serious inadequacies. The PV-ESU-EV coordination along with snubbers in the isolated bidirectional converters is mostly the focus of solutions for decentralized control of islanded EV charging infrastructure. However, it has received little attention as shown in the small number of published research work. Unfortunately, the adoption of PV-ESU-EV systems has been significantly hampered by the restricted access to charging infrastructure and growing driving range anxiety. Additionally, societal, and political constraints impede the advancement of these technologies in the general market, particularly in developing nations where there is a wide range of application. Meanwhile, several in-depth studies have been conducted in recent years to address the problems related to the adoption of PV based charging infrastructure installations by using a variety of charging system designs. Since it is stated that the night

is darkest before the sunrise, filling the dispersed PV-ESU-EV infrastructure appears to be the best alternative for boosting economic growth, generating jobs, promoting sustainability, and improving climatic conditions.

The DC system is disconnected from the network, thus more sophisticated management techniques must be utilized to keep the system stable in the face of erratic operating situations such as unexpected ESU disconnections or sharp fluctuations in the PV generating power owing to irradiance. The controllers of the converters should therefore be able to maintain coordination among them and handle these transients through combined droop and master-slave control scheme. Although both droop control and master control can deliver precise current sharing under steady-state and transient situations, the fundamental disadvantage of both control methods is that the ESU is crucial to the stability and dependability of the overall system.<sup>26</sup> In this regard, sluggish charging circumstances are not acceptable for the charging/discharging controller, as it cannot switch off the ESU, nor can it regulate the current through it based on the SOC value falling below or rising above a certain level. A fast disturbance in the system makes it impossible for the EVs to connect to the bus frequently and disconnect from it within a brief period of time. EVs may suffer harm in this operating mode, so a control scheme that takes advantage of both the droop control system and the master-slave control system is proposed to overcome this issue.

This paper describes a PV-based EVCS using droop and master-slave control techniques to maintain system stability by coordinating PV arrays, EVs, and ESU. The present work also proposes an ESU that includes an isolated bidirectional DC-DC converter with passive and active snubbers. This configuration effectively achieves zero-voltage switching conditions across the switches leading to an enhanced performance of the PV-based EVCS. Moreover, it is economical and reliable to have a single snubber circuit topology in the EVCS rather than one in each EV. It was proposed by Huang et al<sup>26</sup> that an off-grid EVCS based on PV arrays, EVs, and ESUs could be coordinated and maintained by a hybrid control scheme. It is designed to maintain stability in the system by employing both the master slave and droop control schemes. There was, however, no capability to achieve zero voltage switching characteristics since they were using a non-isolated bidirectional DC-DC converter. This will very certainly reduce the EVCS's overall efficiency. Furthermore, there are relatively no data from studies concerning a snubber-based bidirectional DC-DC converter in conjunction with a master-slave as well as droop control technique for the implementation of an EVCS. Thus, in this paper, an isolated bidirectional DC-DC converter with active and passive snubber circuits and a

master - slave control scheme combined with a droop control scheme to reduce the impact of circulating current on the main switches is proposed. In addition, the proposed technique can clamp voltage spikes across those switches to achieve maximum efficiency. The combination of droop and master-slave control technique for the PV-based EVCS and the snubber circuits attain minimal voltage fluctuation in the DC bus voltage, thus enabling the ESU to slowly access the maximum allowable number of charge/discharge cycles, thereby enhancing the service life. The proposed work is simulated and validated through MATLAB/Simulink.

In summary, the objectives of the proposed work are:

- Developing a stand-alone off-grid EVCS is a plausible way to promote EV adoption all around the world while minimizing the impact on the present power grid and a considerable decrease in CO<sub>2</sub> emissions.
- Designing the charging station components with the help of derived equations and the control strategies.

## 2 | DC OFF-GRID STRUCTURE

The DC off-grid system fed by a photovoltaic system uses droop and master-slave control schemes that coordinate PV, EVs, and ESU. In addition, a battery storage system is utilized to offer off-grid electricity continually. When the PV arrays' power is limited, the battery storage system steps in to fill the gap. On the other hand, when the amount of solar power generated exceeds the amount required for off-grid operation, the battery is used to store the extra power. Figure 1 shows the overview of the PV-based off-grid EVCS architecture.

### 2.1 | System power and energy analysis

Energy and power relations are calculated during the design process to aid in the development of the system.<sup>27,28</sup> Specifically, the following premises are made:

- The initial energy of the storage battery is “ $E_t$ ” in watt-hour (Wh).
- The amount of solar power “ $P_{PV}$ ” emitted from a PV panel changes with time and is determined by:

$$P_{PV} = \frac{P_{mpp}}{36} (36 - t^2) \quad (1)$$

where  $P_{mpp}$  is the maximum output power from the PVs and “ $t$ ” is the time in hours. In Figure 2, the origin of the time axis of the chart is usually set at noon that is when the irradiation level is at its maximum.<sup>27</sup> A 12-hour period of solar energy is assumed to begin at 6:00 AM and to end at midnight. According to the principle of power balance, the power consumption of EV,  $P_{EV}$  is given by,

$$P_{EV} = P_{PV} - P_{BATTERY} \quad (2)$$

where  $P_{BATTERY}$  is the instantaneous battery power.

The average battery power is assumed to be zero during a day ( $T = 24$  hours).

Hence,

$$\int_0^T P_{BATTERY} dt = 0 \quad (3)$$

Therefore,

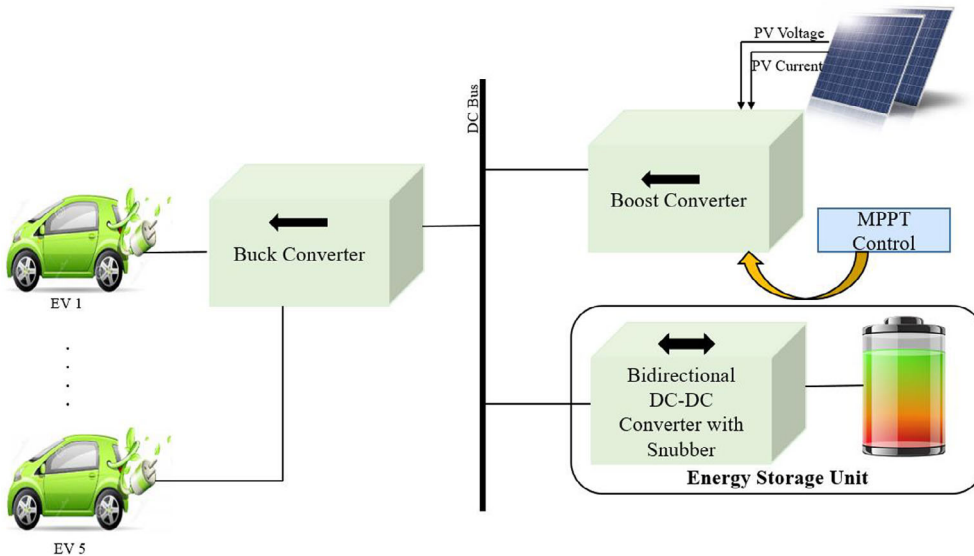


FIGURE 1 Architecture of the off-grid EVCS

FIGURE 2 PV power distribution for a day<sup>27</sup>

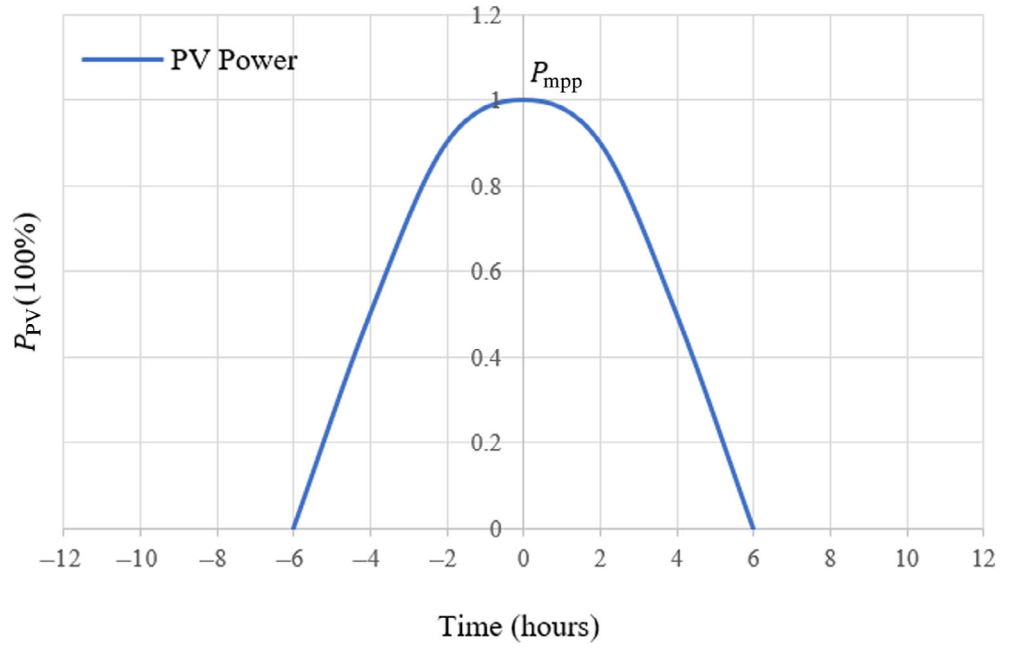
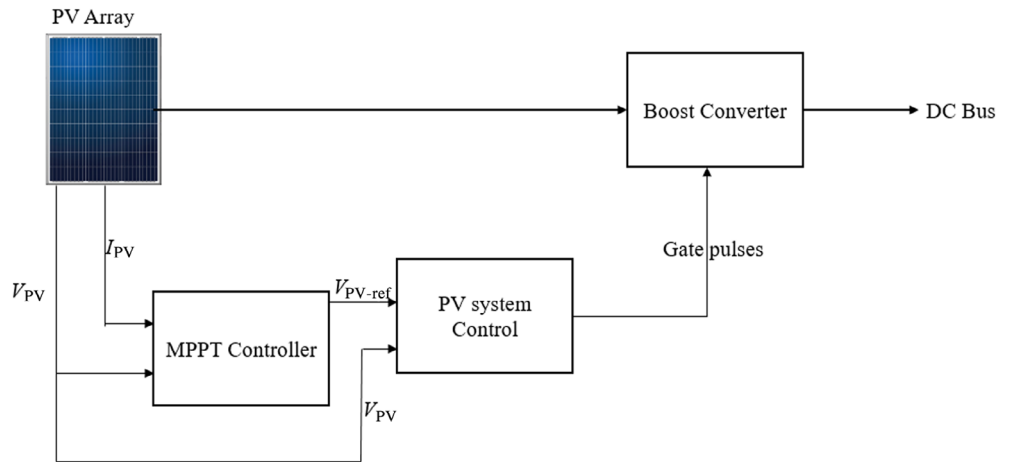


FIGURE 3 Block diagram of PV system control<sup>29,30</sup>



$$\int_{-6}^6 \left[ \frac{P_{mpp}}{36} (36 - t^2) - P_{EV} \right] dt - \int_6^{18} P_{EV} dt = 0 \quad (4)$$

$$P_{mpp} = 3P_{EV} \quad (5)$$

The EV charging station is designed to charge 5 EVs simultaneously. A DC-DC boost converter connects the PV system to a 400 V DC bus. An isolated bidirectional DC-DC converter with an active and passive snubber assists power transfer between the battery and the PV system. The ESU includes a battery storage system and an isolated bidirectional DC-DC converter with an active and passive snubber that can store and release energy which is accomplished by maintaining the DC bus voltage within a reasonable range regardless of the conditions under which it is used. The PV system, which consists of two panels each with 50 kW of electricity, is

the primary energy source for the DC off-grid system, providing a total of 100 kW. The PV system's maximum power is actively monitored and transferred to the DC bus. The ESU stores/releases energy from the PV system with a maximum capacity of 80 kW. The charging station's power consumption is around 24 kW.

## 2.2 | PV panel with a boost converter

The link between the solar array and the DC bus is provided by a three-level boost converter. The maximum power point tracking (MPPT) mode is used by the PV boost converter. The PV system's MPPT control architecture is shown in Figure 3. Using the Incremental Conductance Method,<sup>29,30</sup> the maximum power point of the PV array is determined by measuring its current and



voltage. The PV voltage traces the optimal operating voltage using a PV system control. The three-level boost converter (Figure 4) consists of an inductor, two IGBTs with antiparallel diodes, two capacitors, and two diodes. Such a converter provides higher efficiency and double voltage gain as compared to a conventional boost converter.<sup>26</sup>

### 2.3 | Energy storage unit converter

The ESU consists of a battery and an isolated bidirectional DC-DC converter with a flyback and passive snubber circuit. The bidirectional converter (see Figure 5) provides the battery charging in buck mode and discharging operation in the boost mode, and provides power for the EV loads.<sup>10,11</sup>

When the PV system's generated power exceeds the needed load power, the ESU's primary function is to charge the battery and discharge the battery when the generated

power is inadequate to charge the EVs. The configuration of the isolated bidirectional converter with flyback and passive snubber circuit significantly lowers the influence of circulating current on the main switches, thus voltage spikes across the main switches are efficiently clamped. The bidirectional converter uses a flyback snubber and two passive capacitor-diode snubbers to mitigate the high current and high voltage stress that occurs at the main switch during turn-on or turn-off transitions. When compared to a converter without snubber circuits, the efficiency of the converter with snubber circuits is superior.<sup>10,11</sup> The converter attains zero voltage switching conditions faster than a converter without the snubber. This design provides improved performance of the off-grid EVCS. Furthermore, using a snubber circuit in EVCS rather of having one in each EV is less expensive and more cost-effective.

### 2.4 | EV charger converter

The buck converter (shown in Figure 6) is the EV charger, which consists of a MOSFET switch, an inductor, a diode, and a capacitor.<sup>26</sup> The charger's primary duties

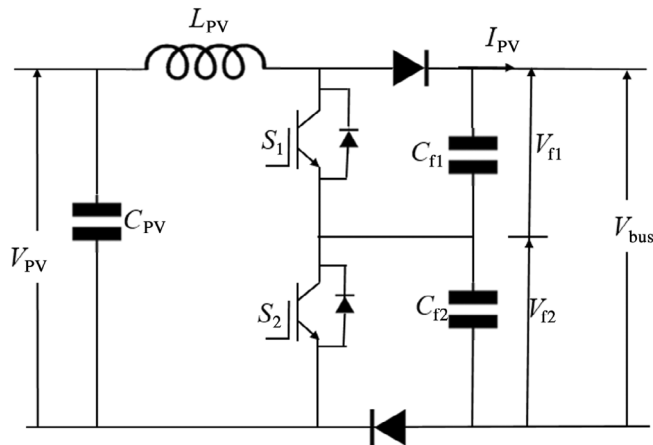


FIGURE 4 PV boost converter<sup>26</sup>

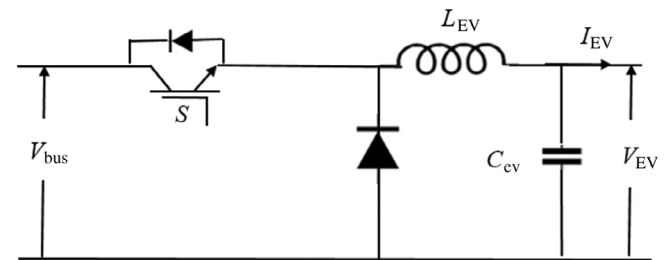


FIGURE 6 EV buck converter<sup>26</sup>

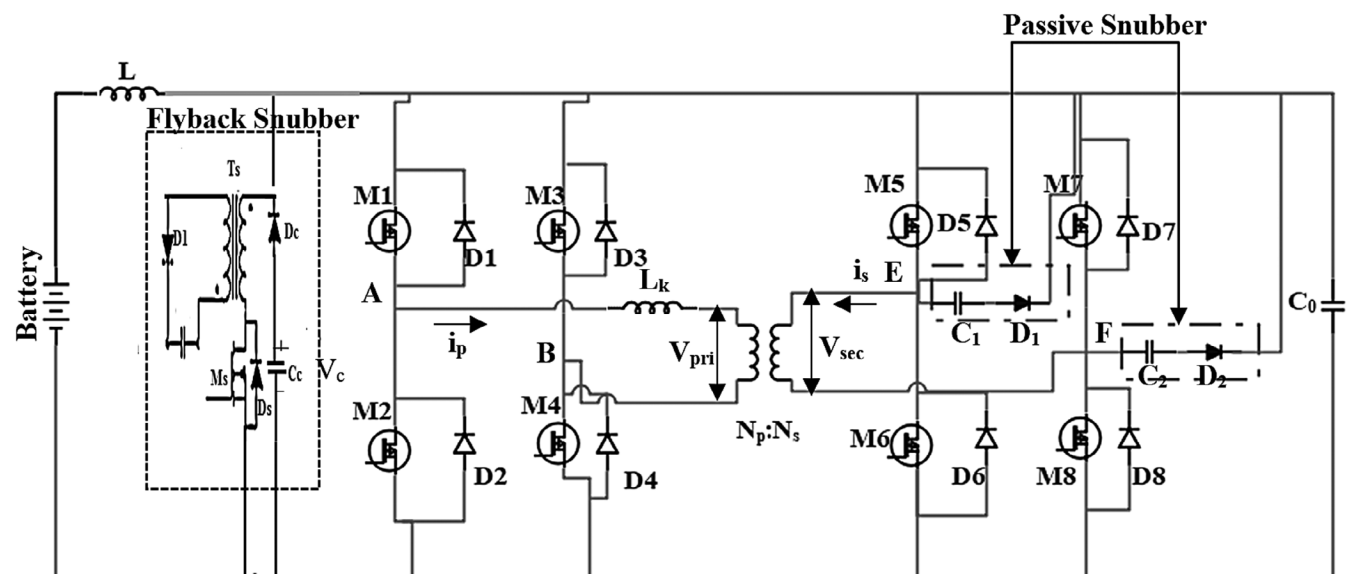


FIGURE 5 Isolated bidirectional DC-DC converter with a flyback snubber and a passive snubber<sup>10,11</sup>

include connecting the DC bus to the EV battery terminals and controlling the charging current. In this work, the charging current is limited to 100A.

### 3 | CONTROL STRUCTURE

The control structure of the DC off-grid system comprises three major algorithms. This includes PV system droop control, ESU converter control, and EV charger converter control and is discussed below in sub-sections.

#### 3.1 | PV system droop control

Through the three-level boost converter, the PV system droop control manages the PV array terminal voltage, extracting the maximum power from the PV arrays. In the PV system droop control, the reference voltage  $V_{PV-ref}$  is obtained from the MPPT algorithm using the Incremental Conductance method.<sup>29,30</sup> The difference between  $V_{PV-ref}$  and  $V_{PV}$  is used to calculate the error term, which is then applied to the proportional-integral (PI) controller to provide the duty ratio,  $D_{PV}$  for the boost converter. This  $D_{PV}$  is then altered by the duty ratio  $D_C$  derived from the error term received as the difference between capacitor voltages of the boost converter,  $V_{f1}$  and  $V_{f2}$ , applied to the secondary PI controller, thereby balancing the two capacitor voltages. Figure 7 shows the control algorithm of the PV boost converter.<sup>26</sup>

#### 3.2 | ESU converter control

The ESU bidirectional converter is controlled to regulate the nominal value of the DC bus voltage,  $V_{bus}$ . The battery is charged and discharged by the ESU converter in boost and buck modes, respectively. Figure 8 shows the flowchart to manage the changeover between the two modes.<sup>26</sup>

There will be continuous monitoring of the reference voltage and bus voltage within the system, which enables the converter's operating scheme to be determined by the contrast between the maximum output power from PVs ( $P_{mpp}$ ) and the maximum consumption from EVs ( $P_{EV}$ ).

The ESU converter control, shown in Figure 9, consists of a reference charging current,  $I_{ESU-ref}$ , and a disable function based on the average sun irradiance,  $G_{avg}$ . This disable function allows to limit the ESU discharging current and to coordinate ESU and EV chargers. All EV chargers are turned off when ESU goes below the minimum state-of-charge (SOC) level and  $G_{avg}$  remains zero until power is generated again by the PV arrays. Since the ESU is so important to the overall system's stability and dependability, it cannot be turned off nor the current through it can be adjusted when SOC goes below or climbs above a specific threshold. However, by combining droop control with the master-slave technology,

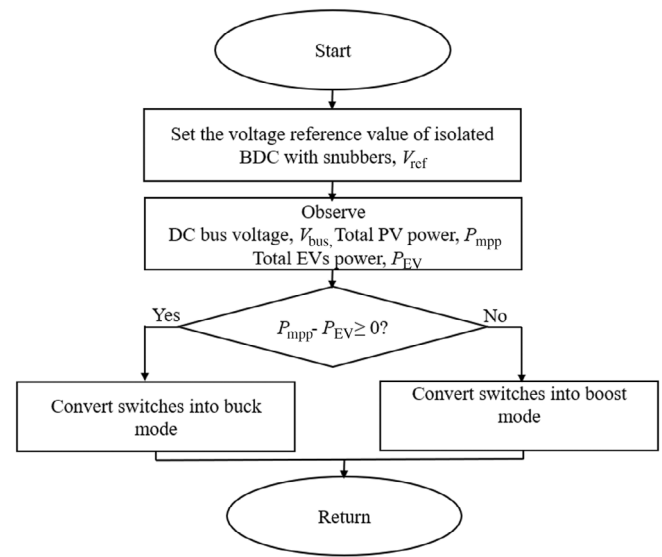


FIGURE 8 Flowchart for the detection of buck/boost mode in isolated bidirectional converter<sup>26</sup>

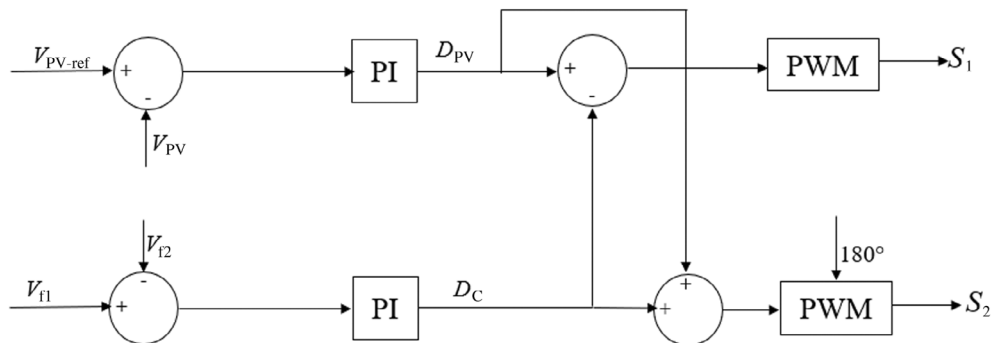
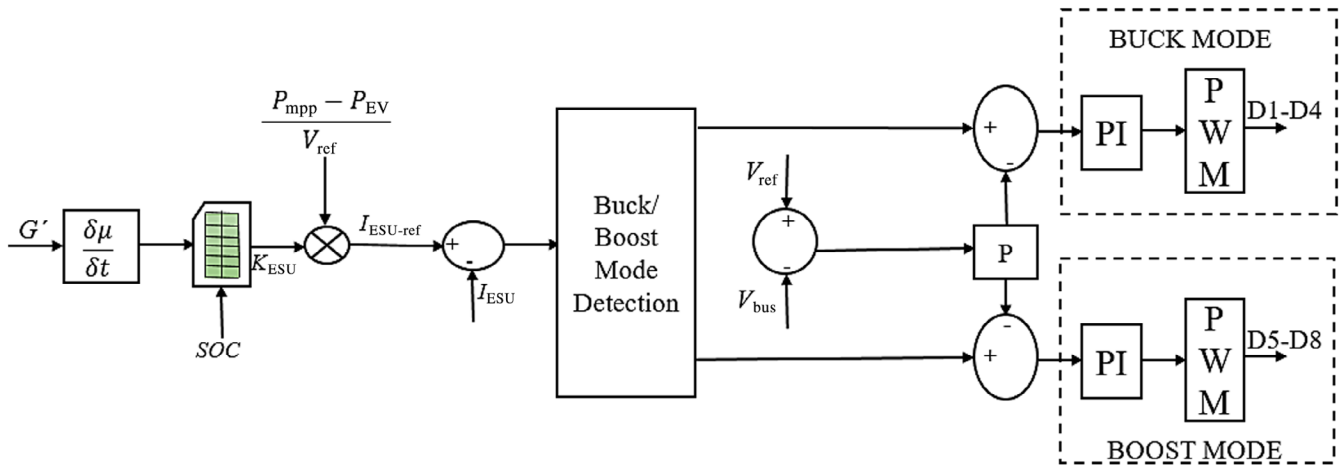


FIGURE 7 Control algorithm of PV boost converter<sup>26</sup>

FIGURE 9 ESU converter control<sup>26</sup>

which provides variable current sharing and great reliability, this flaw may be solved. Therefore, the additional droop control adapts to the slope of solar irradiance  $G' \left( \frac{dG_{avg}}{dt} \right)$ , changes in  $SOC$ , and the demand. The updated storage current reference  $I_{ESU-ref}$  can then be computed as follows:

$$I_{ESU-ref} = \frac{P_{mpp} - P_{EV}}{V_{ref}} \times K_{ESU} \quad (6)$$

where  $K_{ESU}$  stands for the ESU droop gain, which ranges from 0 to 1. The droop gain is calculated using a look-up table depending on  $G'$  and  $SOC$  levels.

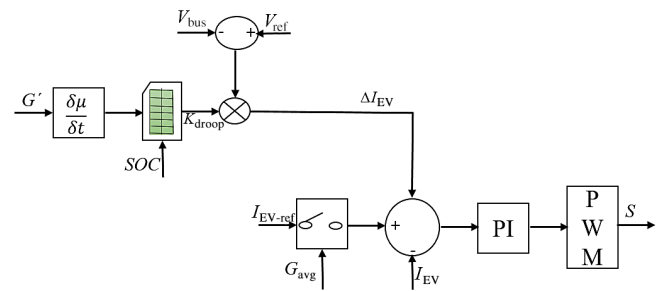
### 3.3 | EV charger converter control

The EV Charger Converter control deploys 5 EVs and a buck converter. The EV charger converter control is shown in Figure 10. The reference charging current is  $I_{EV-ref}$ . The disable function is controlled by the controller based on the average value of solar irradiation,  $G_{avg}$ . The disable function is activated when  $G_{avg}$  falls below a particular threshold, thereafter  $I_{EV-ref}$  approaches zero, and the charger gently disconnects from the DC bus.

The number of unconnected EVs rises as  $G_{avg}$  drops. Figure 9 shows the EV Charger converter control in which the EVs are provisioned with a voltage-based droop control structure. This EV charger converter control regulates the DC-bus voltage. The droop control's output,  $\Delta I_{EV}$  may be stated as follows:

$$\Delta I_{EV} = K_{droop}(V_{ref} - V_{bus}) \quad (7)$$

Where  $K_{droop}$  represents the EVs adaptive droop gain calculated from  $G'$  and  $SOC$ .

FIGURE 10 EV charger converter control<sup>26</sup>

### 3.4 | Modes of operation

**Mode 1:**  $P_{mpp} > P_{EV}$  and  $K_{ESU} = 1$ ,  $K_{droop} = 0$ ,  $SOC$  and  $G'$  are within the specified limits.

If the PV panels' provided power exceeds the necessary power of all connected EVs, the EVs are solely charged from the PV panel. The isolated bidirectional DC-DC converter charges the battery with excess power from the PV panel. The surplus energy may be used for a variety of applications (both domestic and commercial).

**Mode 2:**  $P_{mpp} < \sim 0$  and  $0 \leq K_{ESU} \leq 1$ ,  $0 < K_{droop} \leq 1$  and  $SOC$  and  $G'$  fall outside the specified limits.

If the PV panels' power output is lower (or nil) than the power required by the EVs for charging during rainy and/or no/low sunlight conditions, the extra required power will be captured from the battery through the isolated bidirectional DC-DC converter while retaining a minimum SOC in the battery.

**Mode 3:**  $K_{ESU} < 1$  and  $K_{droop} = 0$  and  $SOC$  reaches the maximum limit.

When no EVs are plugged into the charging station and the battery charging reaches its SOC maximum limit of 90%, the PV panels are unplugged from the bus to preserve the overall system stability.



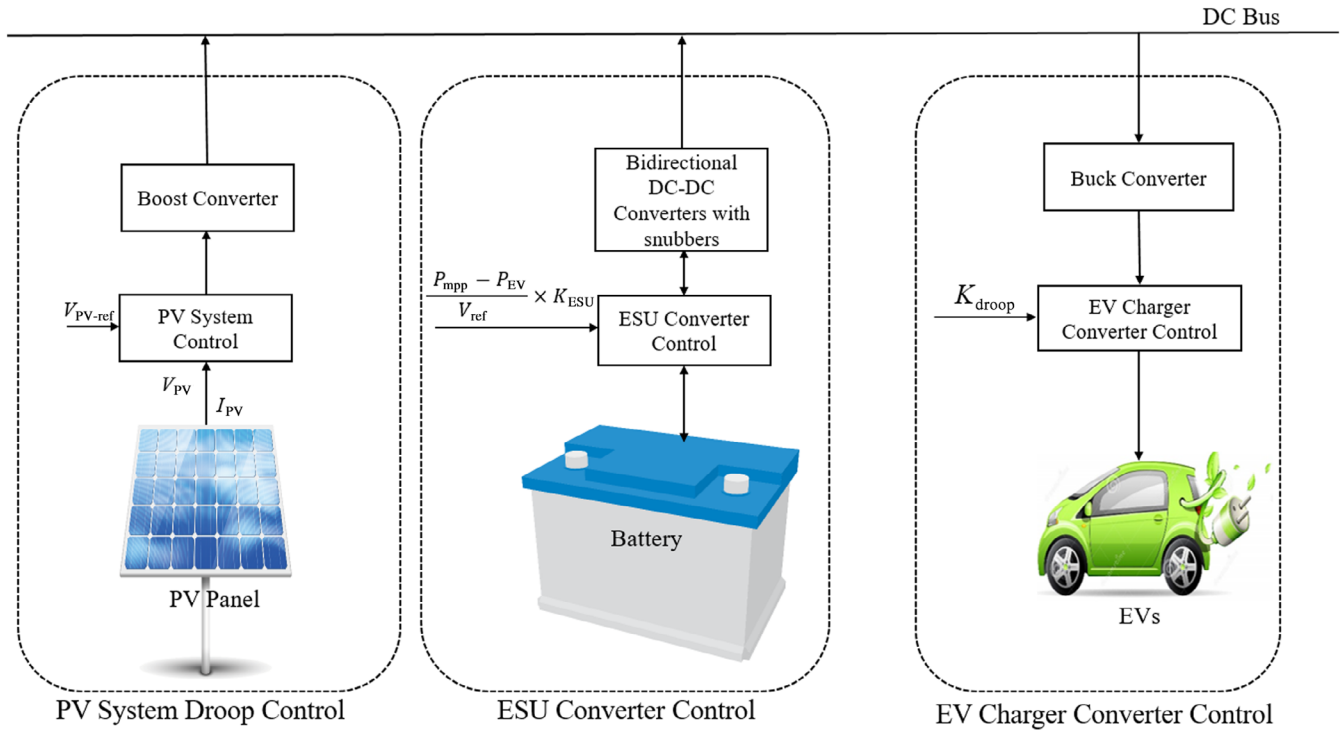


FIGURE 11 Schematic view of the overall control strategy of the off-grid EVCS

Thus the EVCS comprises PV system boost converter droop control, EV charger buck converter droop control and ESU isolated bidirectional converter using both droop and master-slave control along with the PV-ESU-EVs coordination.

## 4 | SIMULATION RESULTS

The system, as shown in Figure 11, is simulated on the MATLAB/Simulink platform, and the simulated results are obtained under different modes of operation.

The battery's initial SOC is set to 20%, with a nominal operating range of 20% to 80%. The PV panels generate the rated electricity initially, with no EVs connected. Therefore the maximum power tracked from the boost converter flows to the ESU. The overall system stability is affected by one of the most important factors, the rate of change of irradiance,  $G'$ . In the proposed work, we consider the irradiance  $G$  as  $1 \text{ kW/m}^2$  at the outset and gradually reduce it to  $600 \text{ W/m}^2$  at 3 s, further drops to  $0 \text{ kW/m}^2$  at 5 s as shown in Figure 12.

### 4.1 | Mode 1

The EV's SOC ranges from 20% to 90%. The solar output in mode 1 is more than the total power required for all EVs, and the battery is charged via an isolated

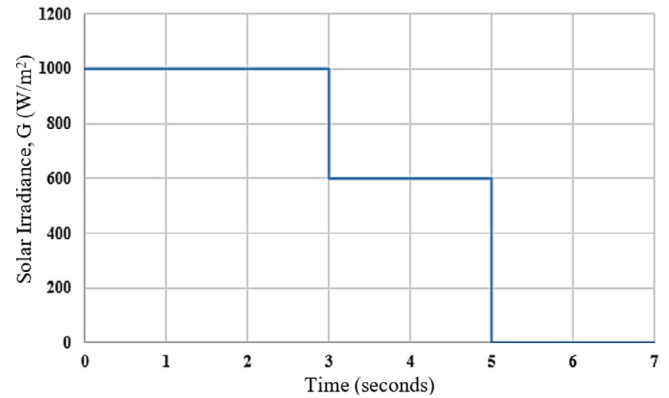


FIGURE 12 Solar irradiance data

bidirectional converter connected to the PV boost converter. Using the extra power from the PV array, the battery is charged until it reaches its maximum SOC. The DC bus voltage is kept constant at 400 V, and the solar array current is 650 A using the droop control and master-slave control. Figure 13 shows the array current drops at  $t = 3 \text{ s}$  when the irradiance falls from  $1 \text{ kW/m}^2$  to  $600 \text{ W/m}^2$ . The current level is similar to the MPPT conditions. In this mode,  $K_{\text{droop}} = 0$  and  $K_{\text{ESU}} = 1$ , and the SOC and  $G'$  are defined within the limits. Therefore, the PV panels provide more electricity than is required for all the EVs, and the excess energy is utilized to charge the battery to its maximum SOC. In Figure 14A, with the

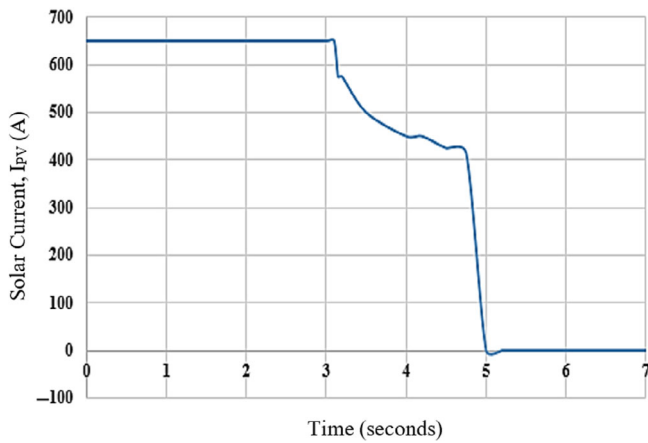


FIGURE 13 Solar array current

surplus ESU power,  $P_{ESU}$ , that is,  $2500\text{ W} - 400\text{ W} = 2100\text{ W}$ , the ESU charges from 20% to 34% SOC (Figure 14B). The battery of EVs will gradually charge from 20%, 30%, 50%, and 70% to 80% SOC are shown in Figure 14C. The current is negative since the EV battery is charging, as shown in Figure 14D.

## 4.2 | Mode 2

As the solar power is less or absent, the battery discharges from the maximum SOC, and this energy is used to charge the EVs as shown in Figure 15A,B. EV charger converter control implements the droop control to maintain the voltage stability. When the change in irradiance  $G'$  exceeds a threshold value and the combined droop and master-slave control is enabled for the ESU converter control, the gain droop,  $K_{droop}$  changes from 0 to 1. The gain  $K_{ESU}$  and  $K_{droop}$  are changed from 1 to 0.9 and 0 to 1, respectively (Figure 15D). Thus the ESU and all linked EVs share the PV power, and the ESU's charging current reduces (Figure 15C).

## 4.3 | Mode 3

When there are no EVs connected, the battery SOC is at its maximum of 90% (Figure 16) with the help of energy from the solar array, and the gain  $K_{ESU} < 1$  and  $K_{droop} = 0$ . The PV panels then get disconnected from the overall system to maintain system stability.

## 5 | COMPARATIVE ANALYSIS

In the proposed PV-based EVCS, ESU plays an important role in stabilizing the DC bus voltage. The ESU's

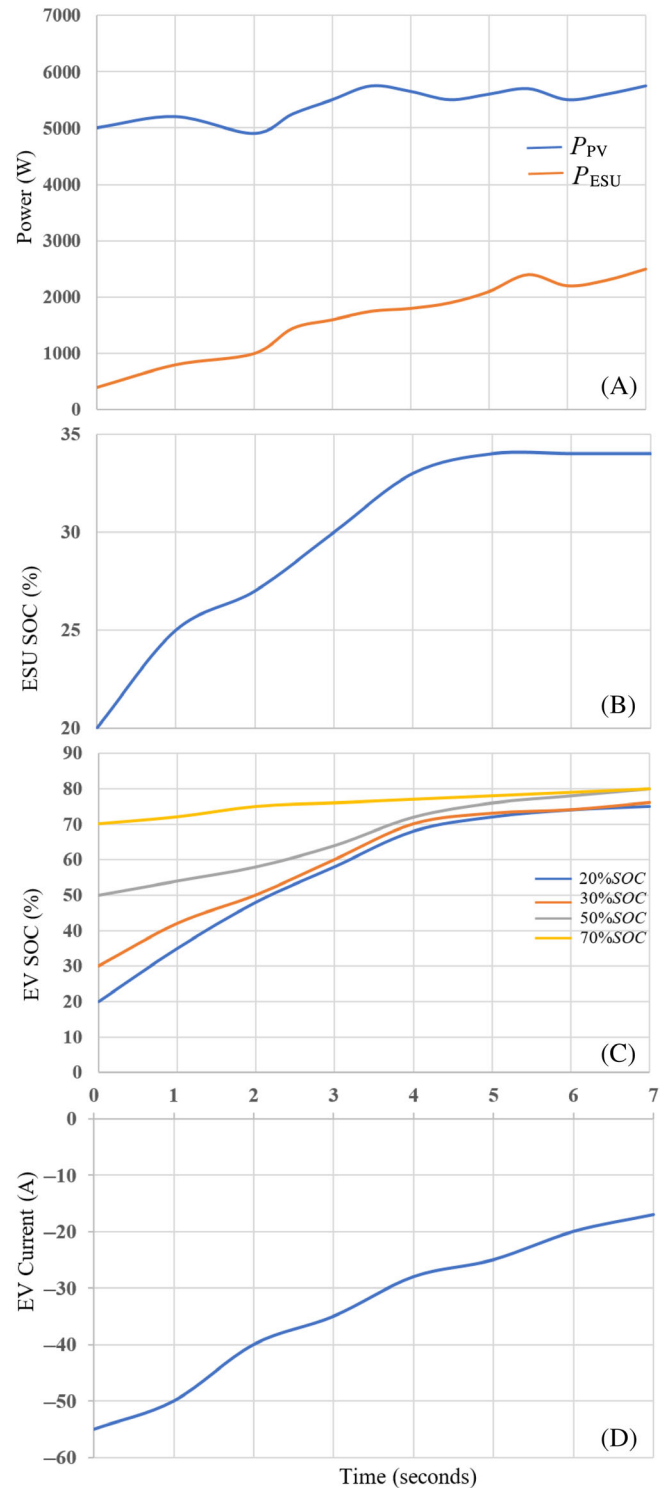
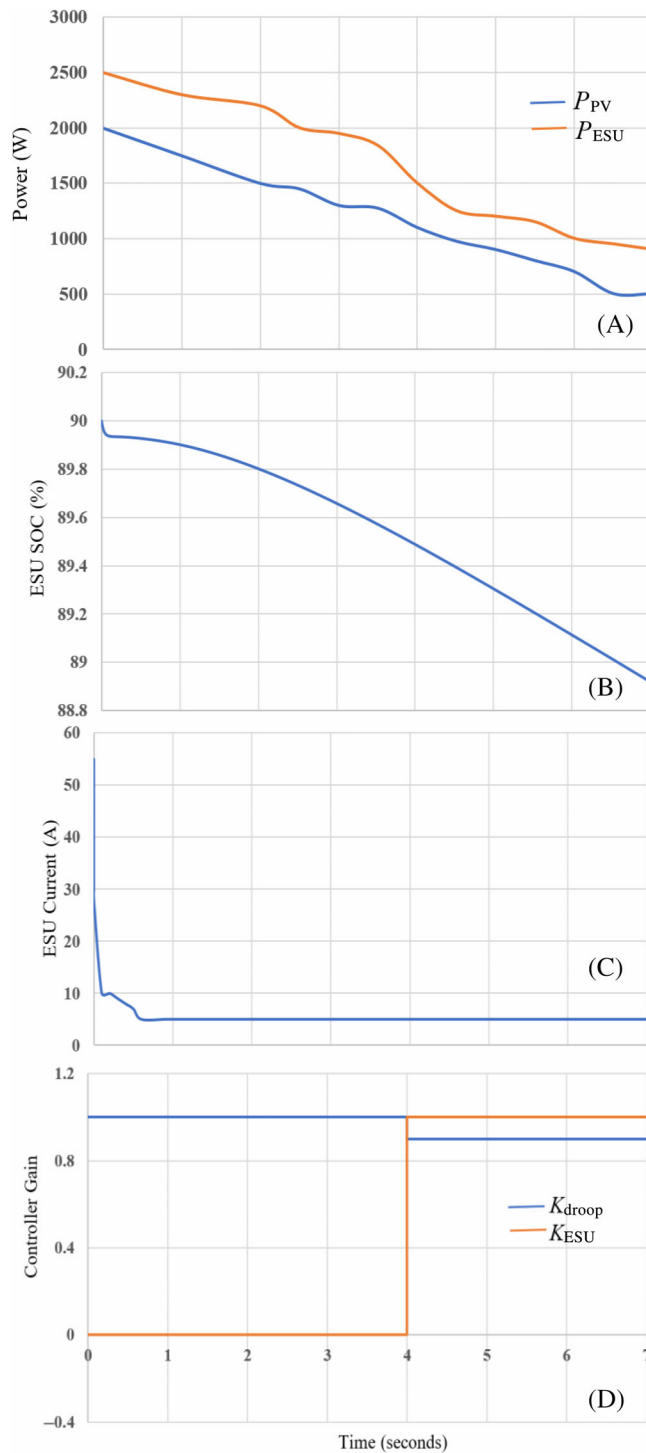


FIGURE 14 A, Solar power and ESU power. B, SOC of ESU. C, SOC of EV charging. D, Current drawn by EV Schematic view of the overall control strategy of the off-grid EVCS

bidirectional converter is designed to keep the voltage level within the certain limits of SOC and  $G'$ . It is insufficient to regulate the voltage or the current through ESU with droop control or master-slave control alone while



**FIGURE 15** A, Solar power and ESU power. B, SOC of ESU. C, Charging current of ESU. D, Controller gain,  $K_{ESU}$  and  $K_{droop}$

SOC is out of the limits. The larger gain of the control techniques causes more voltage deviation. To address the aforementioned problems, an extra control loop is necessary. Hence we implement both control techniques in the proposed PV-based EVCS which utilizes the merits of both droop and master-slave control techniques.

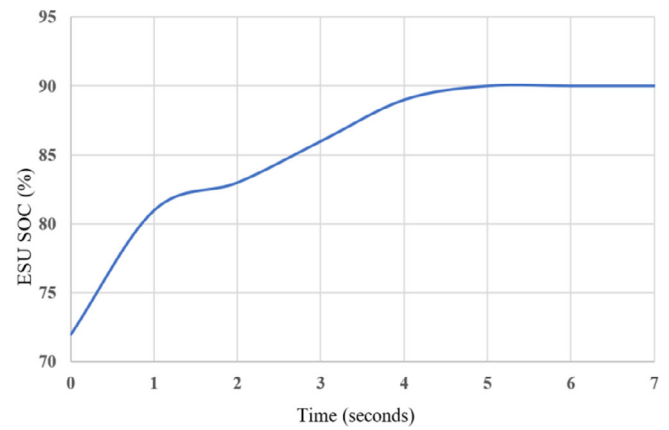


**FIGURE 16** SOC of ESU

Figure 17A,B depicts DC bus voltage variations with master-slave control and droop control with active and passive snubber circuit in the proposed work alone, respectively. The DC bus voltage is shown in Figure 17C using a combination of master-slave and droop control approaches with active and passive snubber circuit in the proposed work. The bus voltage shifts down from the rated value while using the master-slave control technique alone or droop control alone. Note the fluctuations in the DC voltage in both these cases. However, the combination of the master-slave and droop control techniques along with active and passive snubber circuit provides a stable and uniform DC bus voltage. The combination of droop and master-slave control technique for the PV-based EVCS achieves the lowest voltage fluctuation in the DC bus voltage, thus enabling the ESU to slowly access the maximum allowable number of charge/discharge cycles, thereby enhancing the service life. Figure 17D depicts the DC bus voltage proposed by Huang et al.<sup>26</sup> Huang et al.<sup>26</sup> reported a failure in achieving a uniform and stable DC bus voltage using a combination of master-slave and droop control techniques without active and passive snubber circuits, despite efforts. As a result, the service quality of ESU is declining over time.

The key device connecting the ESU and the DC bus is the bidirectional converter requiring a stable, reliable, and efficient topology. However, the bidirectional converter used by Huang et al.,<sup>26</sup> results in significant voltage and current spikes during the connect/disconnect of the EVs to the system frequently. Moreover, the freewheeling current raises conduction losses and reduces the effective duty cycle. These problems are overcome with the help of an isolated bidirectional converter with active and passive snubber circuits in this paper. This converter achieves zero-voltage switching conditions quickly and effectively clamps the voltage spikes across the switches

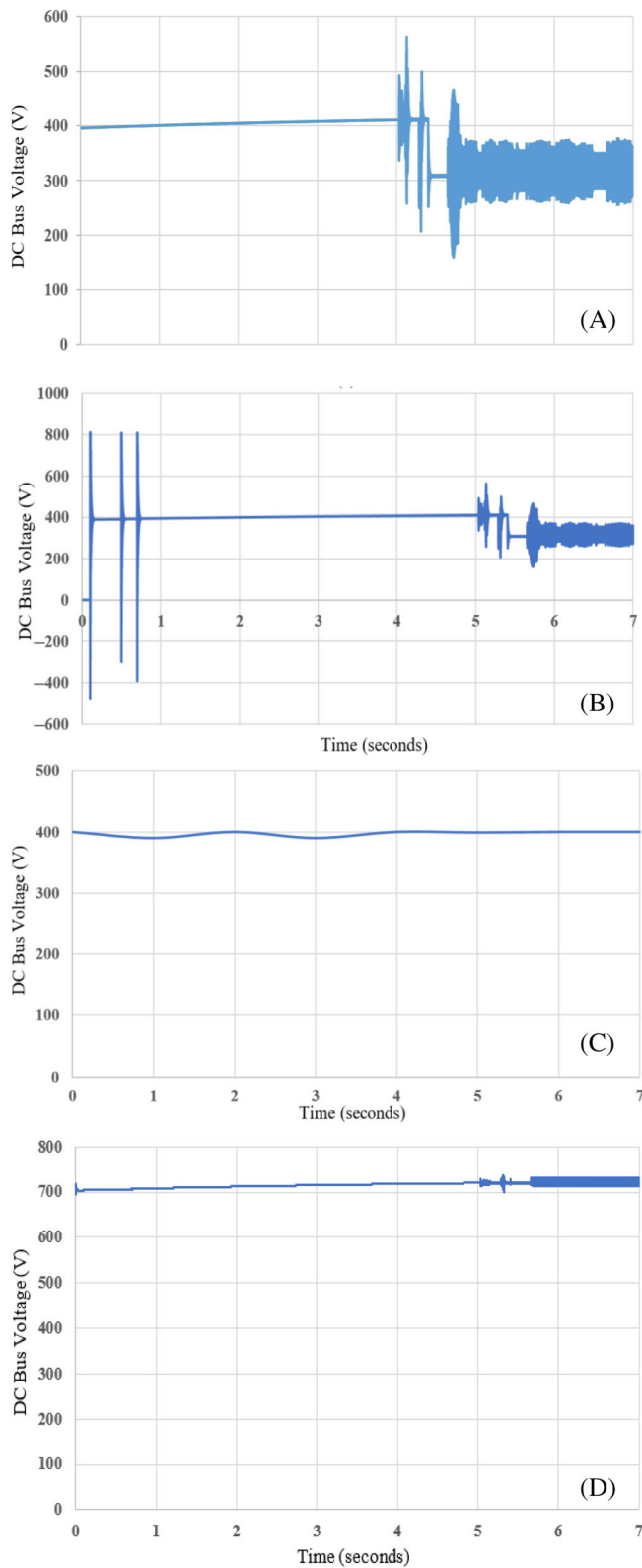


**FIGURE 17** A, DC Bus voltage with master-slave control with active and passive snubber circuit in the proposed work. B, DC Bus voltage with droop control with active and passive snubber circuit in the proposed work. C, DC Bus voltage with the combination of master-slave and droop control with active and passive snubber circuit in the proposed work. D, DC bus voltage without active and passive snubber circuit used by Huang et al<sup>26</sup>

as compared to the bidirectional converter used by Huang et al,<sup>26</sup> thus improving the total efficiency of the PV-based EVCS.

Figure 18A,B shows the clamp branch voltage across the switches of the bidirectional converter used by Huang et al<sup>26</sup> and this work, respectively. It is clear from Figure 18A that the bidirectional converter used by Huang et al<sup>26</sup> creates high voltage stress across the switch, due to the presence of an inductor and does not attain zero-voltage switching conditions. However, in Figure 18B, the usage of an isolated bidirectional converter with snubber circuits in this work attains zero-voltage switching conditions instantaneously within a fraction of seconds. Thus, the isolated bidirectional converter with snubber circuits is the best option as it achieves zero-voltage switching by alleviating the voltage stresses across the main switches. It can be concluded from the above scenarios that the proposed off grid EV charging station utilizing PV generation will be competent to charge EVs under any conditions. Snubber circuits are used in the bidirectional DC-DC converter to ensure that the charging station is as energy-efficient as possible and to safeguard the system from high voltage and high

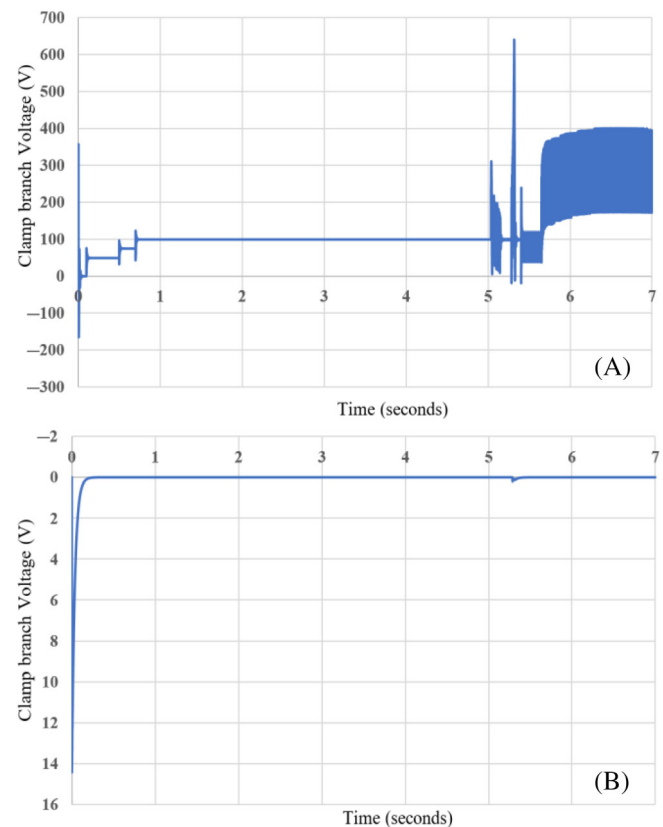


**FIGURE 18** A, Clamp branch voltage of the bidirectional converter used by Huang et al.<sup>26</sup> B, Clamp branch voltage of the isolated bidirectional converter with active and passive snubber circuits in this work

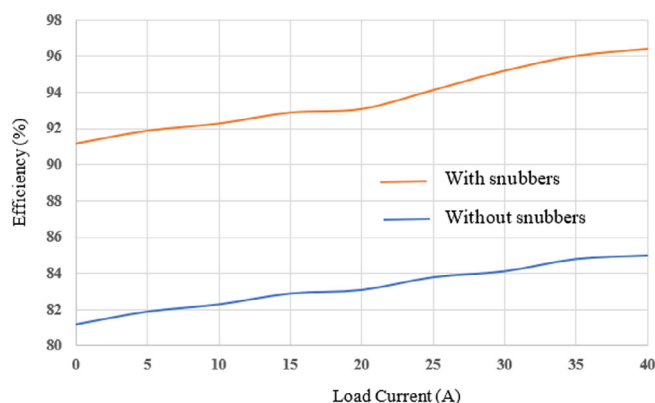


**FIGURE 19** Plot of conversion efficiency of the proposed work

current strains. By keeping the input voltage constant, the efficiency curve is produced. With a fixed amount of input voltage of 400 V, Figure 19 displays the efficiency curves for inductor current fluctuation ranges of 2 to 40 A. As a result of the occupancy advantages of active and passive snubber circuits coupled with dual control schemes, the maximum efficiency of a bidirectional DC-DC converter without a snubber circuit is approximately 85%, whereas the highest efficiency of a bidirectional DC-DC converter with an active and passive snubber circuit combined with dual control schemes is 96.4%. Consequently, with active and passive snubber circuits, the bidirectional DC-DC converter achieves a higher efficiency than the bidirectional DC-DC converter without snubber circuits, in that the latter achieves lower efficiency.

## 6 | CONCLUSION

The paper proposes a combination control scheme for a PV-based EVCS with improved system stability as compared to a conventional master-control only or conventional droop control scheme only. The three-level boost converter designed to provide higher efficiency for PV generation is controlled by incremental and conductance MPPT and a capacitor voltage balance controller. The control schemes for the EV chargers and ESU with an isolated bidirectional DC-DC converter along with active and passive snubbers are also described. The combination of droop control and master-control scheme with active and passive snubber circuits maintains the DC bus voltage stable and constant at 400 V while obtaining the desired power. The proposed station's design is validated using MATLAB/Simulink, taking into account three alternative modes of EV operation. The design and control scheme is shown to be robust. The EVCS were also

compared in terms of performance. The isolated bidirectional converter with snubber circuits achieves zero-voltage switching conditions more rapidly as compared to the converter without snubber circuits. This will enhance the system's reliability. An outstanding solution for PV-dependent EV charging stations with a conversion efficiency of 96.4% is provided by the combination of active and passive snubbers with a bidirectional DC-DC converter, a dual control system with master slave droop control technique, and an energy storage device. Using solar energy to electrify road transportation as well as deploys them in remote rural areas without access to the grids is within the scope of the proposed design.

There have been a number of observations made in the proposal that have been discussed below:

- EVCS based on DC supply technology is more suitable since there is less conversion loss involved.
- The charging station's ESU enables the efficient use of solar energy while ensuring that EVs can charge continuously.
- Through the use of master-slave and droop control techniques along with snubber circuits in the control of the EVCS, fast charging and discharging of the batteries can be accomplished as well as better regulation of DC bus voltages can be achieved.

By implementing new technologies for charging EVs, such as off-grid EVCS, smart charging techniques, electric vehicle control systems, and many more, a balance will be maintained in the energy sector, which in turn will maximize the use of renewable energy such as solar energy. Additionally, it will assist in communicating with the clients and ensuring that they are satisfied in addition to ensuring cost-effective charging rates. An optimized charging system will reduce the charging time for EVs, along with a stable DC bus voltage, which is very crucial for the efficient operation of the charging infrastructures for EVs. It is possible to promote a stable DC based off-grid EVCS system with the highest energy generation from renewable energy sources soon to meet the goals of reducing the dependency on fossil fuels. In addition, it can achieve zero emissions of environmentally harmful gases to provide electricity to expanding and dynamic electrical loads, such as the increasing popularity of electric vehicles.

## ACKNOWLEDGMENT

The authors acknowledge gratefully for the support of School of Engineering, Computer and Mathematical Sciences, Auckland University of Technology, Auckland, New Zealand. Open access publishing facilitated by Auckland University of Technology, as part of the Wiley -



Auckland University of Technology agreement via the Council of Australian University Librarians.

## DATA AVAILABILITY STATEMENT

The data that support the findings of this study are available from the corresponding author upon reasonable request.

## ORCID

Divya Krishnan Nair  <https://orcid.org/0000-0001-7416-4188>

## REFERENCES

- Daza, JSO, Cristancho ACB, Restrepo M, Arango-Manrique A. Application software for studying the impact of electric vehicle charging stations in distribution systems. 2021 IEEE PES innovative smart grid technologies conference—Latin America, ISGT Latin America 2021 (2021). doi:10.1109/ISGTLATINAMERICA52371.2021.9543084
- Electric Vehicles – Analysis - IEA. <https://www.iea.org/reports/electric-vehicles>. Accessed December 5, 2022.
- Grasel B, Baptista J, Tragner M. Supraharmonic and harmonic emissions of a Bi-directional V2G electric vehicle charging station and their impact to the grid impedance. *Energies*. 2022;15:2920.
- Paul Sathiyam S, Pratap CB, Stonier AA, et al. Comprehensive assessment of electric vehicle development, deployment, and policy initiatives to reduce GHG emissions: opportunities and challenges. *IEEE Access*. 2022;10:53614-53639.
- Sheng K, Dibaj M, Akrami M. Analysing the cost-effectiveness of charging stations for electric vehicles in the U.K.'s rural areas. *World Electr Veh J*. 2021;12:232.
- Mamidala S, Prajapati AK, Ravada S. Modeling of buck converter charging station to improve the power quality using three phase single tuned harmonic filter for electric transportation. Paper presented at: 2022 IEEE 2nd International Conference on Sustainable Energy and Future Electric Transportation, SeFeT 2022, Institute of Electrical and Electronics Engineers Inc., 2022. doi:10.1109/SeFeT55524.2022.9909306
- Zou Y, Zhao J, Gao X, Chen Y, Tohidi A. Experimental results of electric vehicles effects on low voltage grids. *J Clean Prod*. 2020;255:120270.
- Wang Z, Jochem P, Fichtner W. A scenario-based stochastic optimization model for charging scheduling of electric vehicles under uncertainties of vehicle availability and charging demand. *J Clean Prod*. 2020;254:119886.
- Girard A, Roberts C, Simon F, Ordoñez J. Solar electricity production and taxi electrical vehicle conversion in Chile. *J Clean Prod*. 2019;210:1261-1269.
- Krishnan Nair D, Prasad K, Lie TT. Standalone electric vehicle charging station using an isolated bidirectional converter with snubber. *Energy Stor*. 2021;3:e255.
- Nair DK, Prasad K, Lie TT. Implementation of snubber circuits in a PV-based off-grid electric vehicle charging station—comparative case studies. *Energies*. 2021;14:5853.
- Dave J, Ergun H, van Hertem D. Incorporating DC grid protection, frequency stability and reliability into offshore DC grid planning. *IEEE Trans Power Deliv*. 2020;35:2772-2781.
- Mathew EC, Das A. A new isolated bidirectional switched capacitor DC-DC converter for exchanging power with MVDC grid. Paper presented at: 2022 IEEE IAS Global Conference on Emerging Technologies, GlobConET 2022 974–980, Institute of Electrical and Electronics Engineers Inc., 2022. doi:10.1109/GlobConET53749.2022.9872374
- Top 5 Off Grid Solar Projects | Zonna Energy | 2022 List. <https://www.zonnaenergy.com/top-off-grid-solar-projects/>. Accessed December 5, 2022.
- Leippi A, Fleschutz M, Murphy MD. A review of EV battery utilization in demand response considering battery degradation in non-residential vehicle-to-grid scenarios. *Energies*. 2022;15:3227. doi:10.3390/en15093227
- Sasikumar G, Sivasangari A. Design and development of solar charging system for electric vehicles: an initiative to achieve green campus. *Nat Environ Pollut Technol*. 2021;20:801-804.
- Ayyadi S, Maaroufi M. Optimal framework to maximize the workplace Charging Station owner profit while compensating electric vehicles users. *Math Probl Eng*. 2020;2020:1-12.
- Azaroual M, Ouassaid M, Maaroufi M. Optimum energy flow management of a grid-tied photovoltaic-wind-battery system considering cost, reliability, and CO<sub>2</sub> emission. *Int J Photocenergy*. 2021;2021:1-20.
- Shariff SM, Alam MS, Ahmad F, Rafat Y, Asghar MSJ, Khan S. System design and realization of a solar-powered electric vehicle Charging Station. *IEEE Syst J*. 2020;14:2748-2758.
- Liemthong R, Srihapon C, Ghosh PK, Chatthaworn R. Home energy management strategy-based meta-heuristic optimization for electrical energy cost minimization considering TOU tariffs. *Energies*. 2022;15:537.
- Tran VT, Islam MR, Muttaqi KM, Sutanto D. An efficient energy management approach for a solar-powered EV battery charging facility to support distribution grids. *IEEE Trans Ind Appl*. 2019;55:6517-6526.
- Thang T, Ahmed A, Kim CI, Park JH. Flexible system architecture of stand-alone PV power generation with energy storage device. *IEEE Trans Energy Convers*. 2015;30:1386-1396.
- Wu D, Tang F, Dragicevic T, Guerrero JM, Vasquez JC. Coordinated control based on bus-signaling and virtual inertia for islanded DC microgrids. *IEEE Trans Smart Grid*. 2015;6:2627-2638.
- Xia Y, Yu M, Yang P, Peng Y, Wei W. Generation-storage coordination for islanded DC microgrids dominated by PV generators. *IEEE Trans Energy Convers*. 2019;34:130-138.
- Mohamed K, Wolde HK, Al-Farsi AMS, Khan R, Alarefi SMS. Opportunities for an off-grid solar PV assisted electric vehicle charging station. Paper presented at: 11th International Renewable Energy Congress, IREC 2020, Institute of Electrical and Electronics Engineers Inc., 2020. doi:10.1109/IREC48820.2020.9310376
- Huang H, Balasubramaniam S, Todeschini G, Santoso S. A photovoltaic-fed dc-bus islanded electric vehicles charging system based on a hybrid control scheme. *Electronics*. 2021;10:1142.
- Atawi IE, Hendawi E, Zaid SA. Analysis and design of a standalone electric vehicle charging station supplied by photovoltaic energy. *Processes*. 2021;9:1246.
- Spertino F, Ciocia A, di Leo P, Malgaroli G, Russo A. A smart battery management system for photovoltaic plants in households based on raw production forecast. <http://www.intechopen.com>. Accessed December 5, 2022.

29. Jagtap S, Khandekar A. Implementation of combined system between perturb observe and incremental conductance technique for MPPT in PV system. Paper presented at: 2021 2nd Global Conference for Advancement in Technology, GCAT 2021, Institute of Electrical and Electronics Engineers Inc., 2021. doi:[10.1109/GCAT52182.2021.9587457](https://doi.org/10.1109/GCAT52182.2021.9587457)
30. Stephen AA, Musasa K, Davidson IE. Modelling of solar PV under varying condition with an improved incremental conductance and integral regulator. *Energies*. 2022;15:2405.

**How to cite this article:** Krishnan Nair D, Prasad K, Lie TT. Design of a PV-fed electric vehicle charging station with a combination of droop and master-slave control strategy. *Energy Storage*. 2023;e442. doi:[10.1002/est2.442](https://doi.org/10.1002/est2.442)